Nuclear Physics B116 (1976) 317–333

DOUBLE EXCHANGE MODEL DESCRIPTION OF THE CHARGE EXCHANGE REACTION $K^-p \to K^*\pi^+n$

Amsterdam–CERN–Nijmegen–Oxford Collaboration

Edmond L. BERGER
Argonne National Laboratory High Energy Physics Division ★

J. VERGEEST ★★
CERN, Geneva

Received 23 August 1976

We formulate a simple doubly peripheral exchange model to describe $K^-p \to K^{*-}\pi^+n$ at small values of the $(K^*\pi)$ invariant mass. The model satisfies the requirements of duality, incorporating exchange degenerate exchanges in both t channels. Our parametrization respects analyticity properties (Steinmann relations) of the two-reggeon single-particle central vertex. At the pion pole in one of the t channels, our model reduces to the usual π exchange Deck model. We compare distributions from the model with high statistics data at 4.2 GeV/c and find reasonable agreement.

1. Introduction

The charge exchange process $K^-p \to (K^{*-}\pi^+)n$ is expected to be valuable for several reasons. From a resonance perspective, it allows the investigation of possible $J^P = 1^+$ resonance production in the Q region, $M(K^*\pi) < 1.5$ GeV, with background conditions which differ significantly from those found in the "diffractive" channels $K^{\pm}p \to (K^*\pi)p$. From the viewpoint of exchange model dynamics, the reaction is interesting because the t-channel exchanges at the nucleon vertex have isospin 1. The pomeron and f_0 are excluded. Since the pomeron is known to have different properties in elastic and inelastic exclusive processes [1], it is useful to deal with processes in which it is absent. The $I = 1$ exchange candidates include ρ, A_2, and π. The π exchange amplitudes provide primarily natural parity $(K\pi\pi)$ final states; e.g. $K^*(1420)$ with $J^P = 2^+$. The ρ and A_2 can produce the unnatural parity states $J^P = 0^-, 1^+, 2^-$

★ Work performed under the auspices of the US Energy Research and Development Administration.
★★ Now at Fysisch Laboratorium, Universiteit van Nijmegen.

and so forth. In this article we are interested in the unnatural parity component, which has been shown [2] to dominate at low mass, $M(K^*\pi) < 1.3$ GeV.

To describe the low subenergy behavior of the $(K^*\pi)$ system, we may invoke the Deck model [3], which has been used widely in attempts to describe diffractive production. For our charge exchange case, the π exchange Deck graph is drawn in fig. 1a. No graph corresponding to fig. 1a exists with the π^+ emitted at the left vertex, because such a diagram would require an exotic exchange with the quantum numbers of $(K^-\pi^-)$. This is one important simplification vis-à-vis the diffractive case $K^\pm p \to (K^{*0}\pi^\pm)p$. In the diffractive case, both (t-channel) π and (u-channel) K^* exchange graphs are *a priori* possible, and experimental distributions indeed show evidence for strong contributions from both [4]. A second theoretical simplification is that the charge exchange Deck graph includes only the relatively well understood trajectories π and ρ. The reggeized pion exchange Deck amplitude corresponding to fig. 1a is given in ref. [3]. Rather than a Regge ρ exchange amplitude for the right-hand side of the diagram, the full $\pi^0 p \to \pi^+ n$ amplitude is used in ref. [3]. This amplitude is reconstructed from πN phase shifts. Various mass, momentum transfer, and angular distributions predicted by this π exchange Deck model were compared with data at 4.2 GeV/c. While angular distributions in the $(K^*\pi)$ decay frame are well reproduced [5], the (production) distribution in momentum transfer $d\sigma/dt_{pn}$ was found to fail seriously in comparison with experiment. The data fall roughly as $\exp(-3t'_{pn})$ whereas the model predicts a steeper distribution $\exp(-7t'_{pn})$. The steep fall-off in the model is a direct reflection of the observed $d\sigma/dt$ for $\pi^- p \to \pi^0 n$. This is the first important conclusion of our study, and it is discussed in more detail in subsect. 2.4.

Inasmuch as the A_2 trajectory may also be exchanged at the nucleon vertex, the

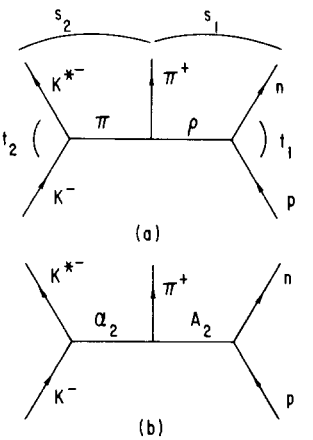

Fig. 1. (a) Pion exchange Deck amplitude for $K^- p \to K^{*-}\pi^+ n$, with ρ exchange at the nucleon (pn) vertex. The kinematic variables used in the paper are also listed. (b) Double exchange graph with A_2 exchange at the pn vertex. The trajectory α_2 is discussed in the text.

graph drawn in fig. 1b must be considered in addition to fig. 1a. Owing to G parity restrictions, the trajectory α_2 in the $K^*\pi$ channel cannot be the π. We require an exchange with positive G which couples to $(K^*\bar{K})$ and to (πA_2). Some candidates are η, B, f, and ρ, whose intercepts are

$$\alpha_\eta(0) \cong \alpha_B(0) \cong -0.3 ,$$

$$\alpha_\rho(0) \cong \alpha_f(0) \cong +0.5 .$$

We may exclude the ρ and f because they should contribute less strongly to the cross section at small $s_2 = M^2(K^*\pi)$. This follows because the cross section contributed by a double-peripheral graph behaves roughly as [6]

$$d\sigma \simeq (s_2/s_1)^{\alpha_2(0)-\alpha_1(0)}\, d\ln(s_2/s_1) .$$

By contrast, the low intercepts of π and B make them efficient generators of cross section at low subenergy. The couplings $(\bar{K}K^*\rho)$ and $(\bar{K}K^*f)$ are also suppressed at small t_2 owing to parity conservation.

Duality arguments, developed in sect. 2, demonstrate the need for both B and η type contributions in fig. 1b. In addition, their relative strengths and phases are prescribed. Duality also relates figs. 1a and 1b so that, in the limit of strict duality, the introduction of fig. 1b is at the expense of no additional parameter.

In our actual calculations, we follow the standard procedure of breaking exchange degeneracy by employing trajectories with their "true" intercepts

$$\alpha_\pi(0) \simeq -0.02 ,$$

$$\alpha_B(0) \simeq -0.3 ,$$

rather than the common intercept suggested by perfect duality. We retain the couplings and phases demanded by exchange degeneracy. The net result is to reduce substantially the magnitude of the (η, B) amplitude, fig. 1b, relative to the π term fig. 1a. The predictions of this new model, which one may term an exchange degenerate reggeized Deck model, agree reasonably with data at 4.2 GeV/c.

The comparison with data at 4.2 GeV/c is discussed in sect. 3, where predictions are also given for other energies. In sect. 4, we draw further implications of our work and summarize our conclusions.

2. Model for $K^-p \to K^{*-}\pi^+n$

2.1. Duality and exchange degeneracy

In a $2 \to 2$ body hadronic reaction, there are in general three topologically different reaction amplitudes which may contribute. These correspond to "exchanges"

in the three pairs of channels (s, t), (s, u) and (u, t). For a general $2 \to 3$ particle reaction as many as twelve topologically different amplitudes may contribute. However, the fact that the $(K^-\bar{n})$, $(K^-\pi^-)$, and $(\bar{p}K^{*-})$ channels are exotic limits us to two graphs for $K^-p \to K^{*-}\pi^+n$. These are drawn in figs. 2a and b. The corresponding high-energy double-Regge-pole approximations to these two amplitudes are drawn below the full amplitudes, in figs. 2c and d. Our interest is in the region of phase space defined by small t_{pn} and small $M(K^*\pi)$. The baryon exchange diagram, fig. 2d, may therefore be ignored.

Because there is only one amplitude remaining in the region of interest, each of the trajectories $\alpha_1(t_1)$ and $\alpha_2(t_2)$ in fig. 2c represents a sum of exchange degenerate trajectories. For example, $\alpha_1(t_1) = \alpha_\rho(t_1) + \alpha_{A_2}(t_1)$. To cancel the contribution from one or the other of these trajectories (i.e. to force a definite signature), one would need to add another graph, similar to fig. 2a, but with the n and p lines rotated about the t-channel axis, as shown in fig. 2e. This graph is forbidden here, since it represents an exotic initial state amplitude.

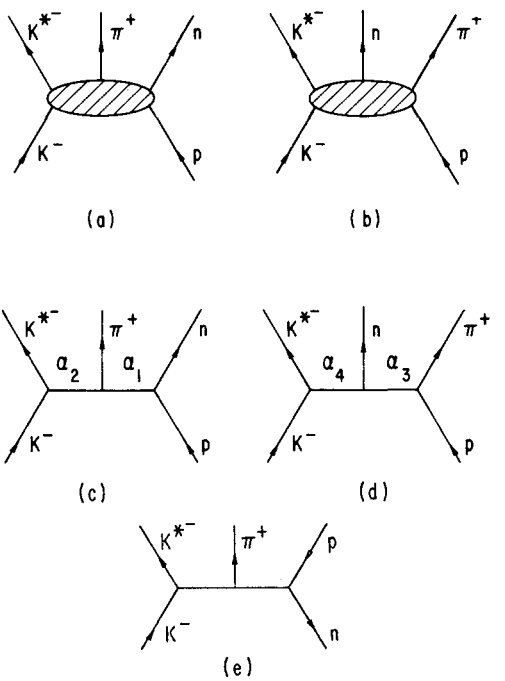

Fig. 2. (a, b) The two topologically distinct five particle amplitudes relevant to $K^-p \to K^{*-}\pi^+n$. Other permutations of the external lines lead to two-particle channels with exotic quantum numbers. (c), (d) The high-energy double exchange graphs corresponding to (a) and (b). The symbols α_1 through α_4 denote Regge trajectories. (e) is obtained from (b) by rotating the p and n lines about α_1.

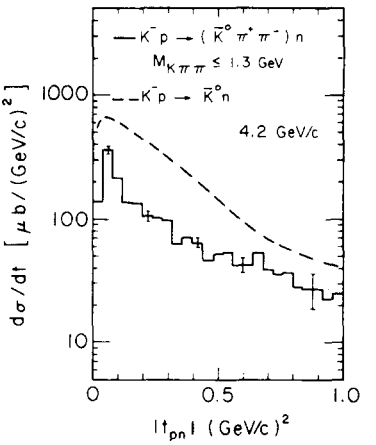

Fig. 3. Comparison of the differential cross sections for the elastic and inelastic charge exchange reactions $K^-p \to \bar{K}^0n$ and $K^-p \to (K\pi\pi)n$ at 4.2 GeV/c. The selection $M(K\pi\pi) \leq 1.3$ GeV is imposed on the inelastic sample. The $\bar{K}^0n$ data are from ref. [11].

The $K^-p \to (K^{*-}\pi^+)n$ situation is thus analogous to the simpler two-body reaction $K^-p \to \bar{K}^0n$, where duality also prescribes a full amplitude in which ρ and A_2 contributions are exchange degenerate. A qualitative indication that the physical situation is quite similar in the elastic and inelastic charge-exchange reactions is provided by fig. 3. Here we compare $d\sigma/dt'_{pn}$ for the two reactions at 4.2 GeV/c. We observe a remarkable similarity in the slopes. Neither distribution shows sign of the pronounced structure near $|t| \simeq 0.5$ (GeV/c)^2, seen in the ρ exchange dominated process $\pi^-p \to \pi^0n$. In $K^-p \to K^0n$, the ρ associated dip seen in $\pi^-p \to \pi^0n$ is filled-in by the A_2 contribution. We pursue the parallel hypothesis here for the inelastic charge exchange process $K^-p \to (K^{*-}\pi^+)n$. Owing to the fact that more particles

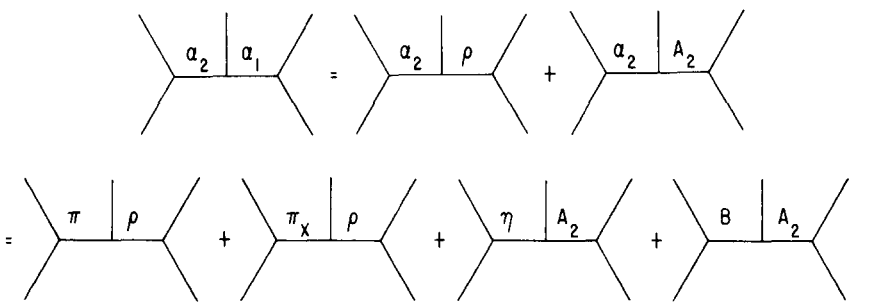

Fig. 4. Decomposition of the fully exchange degenerate amplitude of fig. 2c into the four diagrams with exchanges of definite signature.

are present in the final state, the specification of the reaction amplitudes is more involved.

Fig. 2c represents a sum of four amplitudes, as shown in fig. 4. Corresponding to the choice $\alpha_1(t_1) = \alpha_\rho(t_1)$, there is a pair of exchange degenerate trajectories $\alpha_2(t_2)$ with negative G parity. The standard Deck model amplitude, with $\alpha_1 = \alpha_\rho(t_1)$ and $\alpha_2 = \alpha_\pi(t_2)$, is the first term on the right-hand side of the last equality in fig. 4. Duality requires the inclusion now of a second amplitude, with $\alpha_1 = \alpha_\rho(t_1)$ and $\alpha_2 = \alpha_{\pi_x}(t_2)$ where π_x is used here to denote the experimentally as yet unobserved $I = 0, G = -1$ member of the $J^{PC} = 1^{+-}$ multiplet. It would have mass given by $1 = 0.9\ (M^2 - M_\pi^2)$, or $M \simeq 1.06$ GeV, if the (π, π_x) trajectory is assumed to have slope $0.9\ (\mathrm{GeV}/c)^{-2}$. Because the π_x mass is large, the (π_x, ρ) amplitude has a relatively small magnitude compared to the (π, ρ) contribution.

For the choice $\alpha_1 = \alpha_{A_2}(t_1)$, there is again a pair of exchange degenerate trajectories $\alpha_2(t_2)$, but now with $G = +1$. The obvious candidates are $\alpha_\eta(t_2)$ and $\alpha_B(t_2)$. The $\eta\pi A_2$ coupling is known via the measured 15% decay rate [7] $A_2 \to \eta\pi$. The decay width for $B \to \omega\pi$ can be used along with (ω, A_2) exchange degeneracy to obtain a value for the $B\pi A_2$ coupling strength. At the $\bar{K}K^*$ vertex, one may use (broken) SU(3) relations to derive the $\bar{K}K^*\eta$ coupling from $\bar{K}K^*\pi$, and the $\bar{K}K^*B$ coupling from $\pi\omega B$. These procedures require perhaps too much confidence in SU(3) relationships for the 0^- multiplet. In this connection, we may also remark that a contribution might be expected from the η' exchange amplitude, in place of or in addition to the η. Thus, we use "η" here in a generic sense, to include a possible η' contribution.

To fix the relative sizes of the four graphs in fig. 4, we follow a different procedure. According to strict duality embodied in fig. 2c, the four trajectories are identical

$$\alpha_\pi = \alpha_{\pi_x} = \alpha_\eta = \alpha_B\ . \tag{2.1}$$

In this limit, $m_\eta = m_\pi$. To accommodate the observed mass splitting in the $J^P = 0^-$ multiplet, we break exchange degeneracy, as described below, be employing different trajectories in our amplitude for the (π, π_x) and (η, B) pairs. This displaces the η away from $t_2 = 0$ and thus reduces the (η, B) contribution substantially relative to (π, π_x). Duality specifies equal values for the overall constant coefficients which multiply each of the four terms in fig. 4. We shall retain this second requirement.

2.2. Parametrization of the amplitudes

The parametrization of the fully exchange degenerate amplitude of fig. 2c is well studied theoretically in the limit of large s. Ours is the first application to data. In general, we may express the amplitude in the form [8]

$$A = e^{-i\pi\alpha_2}\,(s/s_2)^{\alpha_1}\, s_2^{\alpha_2}\, \tilde{V}_1(t_1, t_2) + e^{-i\pi\alpha_1}\,(s/s_1)^{\alpha_2}\, s_1^{\alpha_1}\, \tilde{V}_2(t_1, t_2)\ . \tag{2.2}$$

The trajectories are $\alpha_2(t_2)$ and $\alpha_1(t_1)$. The vertex functions $\tilde{V}_1$ and $\tilde{V}_2$ are functions

of t_1, t_2, and $\eta_{12} = s/s_1 s_2$, all phases having been extracted properly. The $\widetilde{V}$'s contain the propagator for the reggeons. We ignore dependence on the Toller angle. As is also true in two-body processes, the t dependences are not fully specified theoretically. Some models are discussed by Brower, De Tar, and Weis [8].

The minimum structure required of $\widetilde{V}_1$ and $\widetilde{V}_2$ is that they exhibit resonance poles at the proper positions: $\alpha_1 = +N_1$ and $\alpha_2 = +N_2$, where N_1 and N_2 are positive integers. Thus, we may try

$$\widetilde{V}_1 = a\Gamma(1-\alpha_1)\,\Gamma(-1+\alpha_1-\alpha_2)\,,$$

$$\widetilde{V}_2 = b\Gamma(-\alpha_2)\,\Gamma(1+\alpha_2-\alpha_1)\,. \tag{2.3}$$

Here, a and b are smooth, slowly varying functions of t_1 and t_2. The function $\widetilde{V}_1$ has resonance poles at $\alpha_1 = N_1 \geqslant 1$. Moreover, when $\alpha_1 = N_1$, $\widetilde{V}_1$ has poles at $\alpha_2 = (N_2 + N_1 - 1)$. A relationship must exist between a and b in eq. (2.3) to ensure that there are no unphysical poles of the full amplitude eq. (2.2) when $(\alpha_1 - \alpha_2)$ equals an integer, but $\alpha_1 \neq N_1$. This can be accomplished if $\widetilde{V}_1$ and $\widetilde{V}_2$ are written in the form of infinite series [8]. In our analysis, we adopt instead simple, reasonable phenomenological forms for these functions.

These expressions are

$$V_1 = \frac{A_0}{(\alpha_1 - 1)(\alpha_2 - \alpha_1 + 1)} \qquad \widetilde{V}_1 = V_1/\eta_{12}\,,$$

$$V_2 = \frac{A_0}{\alpha_2(\alpha_1 - \alpha_2 - 1)} \qquad \widetilde{V}_2 = -V_2\,. \tag{2.4}$$

Here A_0 is an overall normalization constant; it is common to both V_1 and V_2 because of the physical requirement that there be no pole in the full amplitude when $\alpha_\pi(t_2) = \alpha_\rho(t_1) - 1$, but $\alpha_\pi \neq 0$. Note that because $\alpha_2 = \alpha_\pi \simeq 0.9(t_2 - m^2)$, the function V_2 is proportional to the usual pion propagator function. In a more complete model, one would insist that V_1 and V_2 also show poles at the recurrence positions $\alpha_2(t_2) = 1(\mathrm{B})$ and $\alpha_1(t_1) = 2(\mathrm{A}_2)$. However, insofar as t dependence in the scattering region ($t_1 < 0$, $t_2 < 0$) is concerned, this extra complexity has essentially no effect on numerical results. We therefore use eq. (2.4) as our recipe for the vertex functions.

Because α_1 always enters as $(\alpha_1 - 1)$, we adopt henceforth the notation

$$\bar{\alpha}_1 = \alpha_1 - 1\,.$$

Collecting terms, we reexpress our amplitude as

$$A = s_1\left[\mathrm{e}^{-i\pi\alpha_2}(s/s_2)^{\bar{\alpha}_1} s_2^{\alpha_2} V_1(t_1,t_2) + \mathrm{e}^{-i\pi\bar{\alpha}_1}(s/s_1)^{\alpha_2} s_1^{\bar{\alpha}_1} V_2(t_1,t_2)\right]. \tag{2.6}$$

The factor s_1 outside the square-brackets reinstates the correct overall dependence of A on the subenergy variable s_1; i.e. $A \sim s_1^{\alpha_1}$.

In order to implement the breaking of exchange degeneracy, it is first necessary to decompose eq. (2.6) into a sum of two terms each of which is a proper amplitude for an exchange of definite signature in the t_1 channel. This decomposition is

$$A = \tfrac{1}{2} s_1 \sum_{\tau_1} \xi_1 [e^{-i\pi(\alpha_2 - \bar{\alpha}_1)} (s/s_2)^{\bar{\alpha}_1} s_2^{\alpha_2} V_1 + (s/s_1)^{\alpha_2} s_1^{\bar{\alpha}_1} V_2], \tag{2.7}$$

$$\xi_1 = \bar{\tau}_1 + e^{-i\pi\bar{\alpha}_1}, \tag{2.8}$$

where $\bar{\tau}_1$ is the signature of trajectory $\bar{\alpha}_1$ ($\bar{\tau}_\rho = +1$, $\bar{\tau}_{A_2} = -1$). As will be noted, the overall constant coefficient multiplying the two terms ($\bar{\tau}_1 = -1$, and $\bar{\tau}_1 = +1$) in eq. (2.7) is fixed to be the same by duality.

For the $\bar{\tau}_1 = -1$ (A_2) term in eq. (2.7), we set $\alpha_2 = \alpha_B$, whereas for the $\bar{\tau}_1 = +1(\rho)$ term, we take $\alpha_2 = \alpha_\pi$. We break exchange degeneracy by setting

$$\alpha_\pi = 0.9(t_2 - m_\pi^2), \tag{2.9}$$

$$\alpha_B = -0.3 + 0.9 t_2 . \tag{2.10}$$

Strict exchange degeneracy would have required equal intercepts at $t = 0$ for π and B. The choices $\alpha_B(0) = -0.3$ and trajectory slope 0.9 nicely accommodate the observed η and B on the exchange degenerate trajectory

$$\alpha_\eta(t_2) = \alpha_B(t_2) . \tag{2.11}$$

It is therefore unnecessary to further decompose the $\bar{\tau}_1 = -1$ piece of eq. (2.7) into its $\tau_2 = \pm 1$ (η, B) components. A similar remark serves for the $\bar{\tau}_1 = +1$ (ρ) term, since we have placed the π and π_x on the same trajectory.

Our final amplitude can then be expressed as

$$A = \tfrac{1}{2} s_1 \xi_\rho [e^{-i\pi(\alpha_\pi - \bar{\alpha}_\rho)} (s/s_2)^{\bar{\alpha}_\rho} s_2^{\alpha_\pi} V_1^{\pi\rho} + (s/s_1)^{\alpha_\pi} s_1^{\bar{\alpha}_\rho} V_2^{\pi\rho}]$$

$$+ \tfrac{1}{2} s_1 \xi_{A_2} [e^{-i\pi(\alpha_B - \bar{\alpha}_{A_2})} (s/s_2)^{\bar{\alpha}_{A_2}} s_2^{\alpha_B} V_1^{BA_2} + (s/s_1)^{\alpha_B} s_1^{\bar{\alpha}_{A_2}} V_2^{BA_2}] . \tag{2.12}$$

Exchange degeneracy breaking in the t_1 channel can be accomplished by selecting different functions for $\alpha_\rho(t_1)$ and $\alpha_{A_2}(t_1)$ and/or by choosing different normalization strengths for $V^{\pi\rho}$ and V^{BA_2} in eq. (2.12). Because the ρ and A_2 trajectories determined from 2-body data have similar intercepts ($\Delta\alpha(0) \simeq 0.1$), and because our numerical results are not sensitive to such minor differences in the t_1 channel, we adopt the simplification

$$\alpha_\rho(t_1) = \alpha_{A_2}(t_1) = 0.5 + 0.9\, t_1 . \tag{2.13}$$

Likewise, we set

$$V^{\pi\rho} = V^{BA_2} . \tag{2.14}$$

Therefore, the only breaking of exchange degeneracy employed here is the trajectory breaking occasioned by the 0^- multiplet mass differences, c.f. eqs. (2.9) and (2.10). We retain exchange degenerate coupling strengths throughout.

The breaking expressed in eqs. (2.9) and (2.10) is very significant numerically. Were the η and π assigned the same mass, the η pole would be very close to the scattering region and the (η, A_2) amplitude would be comparable in magnitude to the (π, ρ) amplitude at small t_1 and t_2. Our displacement of the η pole to its physical location $t_2 \simeq +0.33$ reduces the net contribution of the (η, A_2) term. Nevertheless, the role of the (η, A_2) term is not negligible, as we will demonstrate numerically in subsect. 2.3.

2.3. Spin

Spin and helicity have been ignored thus far in this article. Because the ρ and A_2 are known to couple dominantly to spin-flip nucleon amplitudes, the easiest way to include this spin effect is to multiply eq. (2.22) by the factor $\sqrt{-t_1}$. From a more realistic treatment, in which both flip and non-flip ρ couplings are extracted from fits to $\pi^- p \to \pi^0 n$, we find $(0.04 - t_1)$ as a multiplicative factor for $|A|^2$.

At the (K, K*) vertex, pion exchange populates dominantly the t_2 channel helicity-0 K* state. We ignore other couplings, for the π as well as for the other three trajectories, and limit ourselves to a description of the dominant t channel helicity-0 K* state.

In order to demonstrate the relative importance of the various contributions to our full amplitude, we have computed $d\sigma/dt'_{pn}$ and $d\sigma/dt_{KK^*}$ for $K^- p \to K^{*-} \pi^+ n$. The integrals over three-body phase space have been performed by Monte Carlo subject only to the restriction $M(K^{*-}\pi^+) < 1.5$ GeV. Here t'_{pn} is the difference $|t_{pn}| - |t_{pn}|_{min}$, where the minimum value of t_{pn} is reevaluated for each simulated event. Distributions are compared in fig. 5 at 10 GeV/c. In this plot, the overall normalization is arbitrary, but the relative normalization between curves is determined by the model. The only "free" parameter in our calculation is the overall normalization constant A_0 which, however, can be determined at the pion pole position from on-shell $\pi^- p \to \pi^0 n$ data and the K* width. We observe that the ρ exchange term $[(\pi + \pi_x)\rho]$ is dominant at small t'_{pn} and t_{KK^*}. In $d\sigma/dt'_{pn}$ the ρ contribution has a "wrong signature" minimum near 0.5 $(\text{GeV}/c)^2$. This dip is completely filled in by the A_2 exchange contribution. The resultant distribution is therefore much less peripheral than the ρ contribution alone. Similar results are obtained at other energies.

2.4. Pion exchange component

From the duality arguments reviewed in detail in subsect. 2.1, we concluded that our full amplitude (eq. (2.12)) is a well-defined sum of four contributions: (π, ρ) +

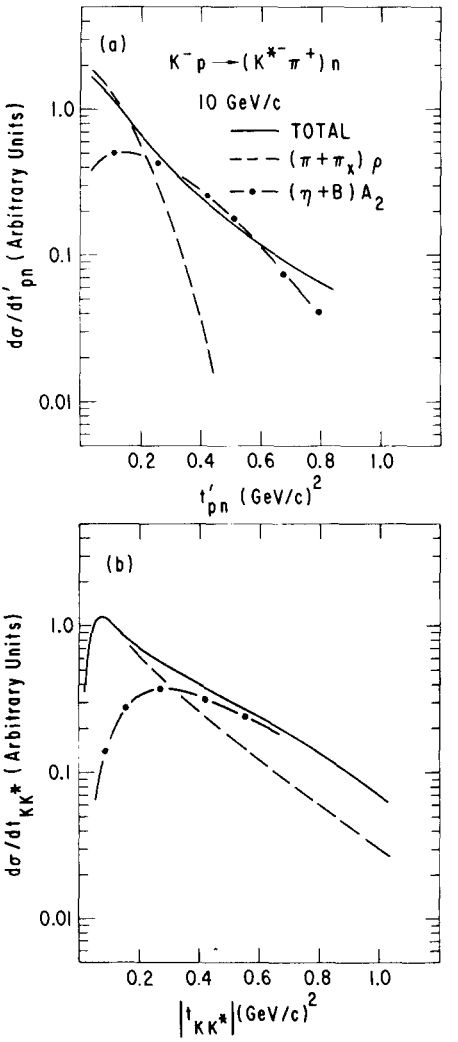

Fig. 5. Predicted differential cross sections (a) in t'_{pn} and (b) in t_{KK^*} for $\mathrm{K}^-\mathrm{p} \to \mathrm{K}^{*-}\pi^+\mathrm{n}$ at 10 GeV/c obtained from our model amplitude eq. (2.12). The integrations are restricted to the region $M(\mathrm{K}^*\pi) \leqslant 1.5$ GeV. Marked are the cross sections obtained if only the $(\pi + \pi_{\mathrm{x}})\rho$ or the $(\eta + \mathrm{B})\mathrm{A}_2$ term is retained in eq. (2.12).

$(\pi_{\mathrm{x}}, \rho) + (\eta, \mathrm{A}_2) + (\mathrm{B}, \mathrm{A}_2)$. The sum contains both positive and negative interference effects, which vary with t_1 and t_2. In the usual π exchange Deck model, one would retain only the $(\pi\rho)$ term. It is instructive to separate this term from the remaining three in eq. (2.12) and to examine its properties. The $\pi\rho$ term is

$$A^{\pi\rho} = \tfrac{1}{4} s_1 \left[\xi_\rho \xi_{\pi\rho} (s/s_2)^{\overline{\alpha}_\rho} s_2^{\alpha_\pi} V_1 + \xi_\pi \xi_{\rho\pi} (s/s_1)^{\alpha_\pi} s_1^{\overline{\alpha}_\rho} V_2\right], \tag{2.15}$$

with

$$\xi_\rho = 1 + e^{-i\pi\bar{\alpha}_\rho}, \tag{2.16}$$

$$\xi_\pi = 1 + e^{-i\pi\alpha_\pi}, \tag{2.17}$$

$$\xi_{\rho\pi} = e^{-i\pi(\bar{\alpha}_\rho - \alpha_\pi)} + 1, \tag{2.18}$$

$$\xi_{\pi\rho} = \xi^*_{\rho\pi}. \tag{2.19}$$

Near the pion pole ($\alpha_\pi = 0$), the second term in square brackets in eq. (2.15) is dominant, and

$$A^{\pi\rho} \to \tfrac{1}{4} A_0 \, \xi_\pi \xi_\rho \frac{s_1^{\alpha_\rho(t_1)}}{\alpha_\pi(\alpha_\rho - 1)}. \tag{2.20}$$

Eq. (2.20) is in fact the simplest expression one would be led to write for the $\pi\rho$ amplitude. It contains the π and ρ propagators, and the proper subenergy dependence $s_1^{\alpha_\rho(t_1)}$. However, eq. (2.15) shows that in extrapolating away from the pion pole, a second term ($\propto V_1$) must be included and that the phase of the pion pole term ($\propto V_2$) is given by $\xi_\pi \xi_{\rho\pi}$ rather than $\xi_\pi \xi_\rho$. These additions are demanded if we are to satisfy analyticity properties of the central $\pi\alpha_\pi\alpha_\rho$ vertex. The V_1 and V_2 terms are equal in magnitude when $\alpha_\pi(t_1) \simeq \alpha_\rho(t_1) - 1$, i.e. for $(t_2 - t_1) \simeq -0.5$, which is well within the region of interest. One important consequence is that in inelastic reactions, the ρ exchange amplitude will not generate the pronounced "wrong signature nonsense" dip in $d\sigma/dt_1$ near $t_1 \simeq -0.5$ (GeV/c)^2 seen in the ρ dominated elastic charge exchange reaction $\pi^- p \to \pi^0 n$. Therefore, for example, in our new approach with proper phase structure, we expect no dip in $d\sigma/dt$ for charge exchange A_1 production. Our conclusions here do not depend on the special forms chosen for V_1 and V_2.

3. Data

In this section, distributions obtained from the exchange degenerate reggeized Deck model described in sect. 2 are compared with data from $K^- p \to K^{*-}\pi^+ n$ at 4.2 GeV/c. While perhaps low in energy, these data are of sufficiently high statistics to allow a detailed comparison of the model with experiment. The experimental statistical sensitivity is 95 eV/μb.

Several tests were performed on the data to ensure that the $K^{*-}\pi^+ n$ sample is pure. First, it is observed that the neutron peak is well separated from the ($n\pi^0$) con-

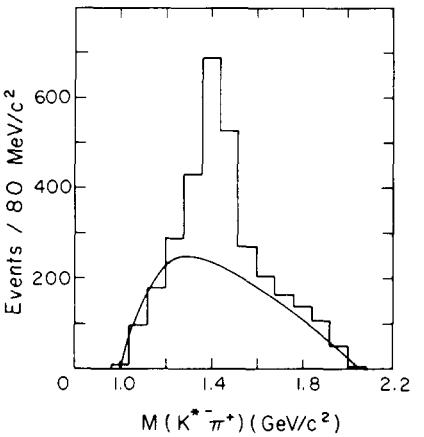

Fig. 6. Distribution in the $(K^{*-}\pi^+)$ invariant mass from $K^-p \to K^{*}\pi^+n$ at 4.2 GeV/c for the sample with $|t_{pn}| \leq 0.8$ (GeV/c)^2. The theoretical curve is obtained from eq. (2.12) of the text and is normalized to the data in the region $M(K^*\pi) \leq 1.28$ GeV.

tinuum. There is thus little contamination from $K^{*-}\pi^+\pi^0 n$ events. Second, at low $M(K^{*-}\pi^+)$, there is a potential kinematic overlap with the K^-pn final state. However, an examination of the $(K^0\pi^-)$ mass plot shows little (~10%) background. All features of the distributions shown here remain unaltered by a K* mass selection broader than the one we adopted ($0.86 < M(K\pi) < 0.94$ GeV). In order to limit ourselves to the peripheral process $K^-p \to (K^{*-}\pi^+)n$, we impose a selection on the value of momentum transfer t_{pn}. As a compromise between strict peripherality and statistics, we chose to work with events having $|t_{pn}| \leq 0.8$ (GeV/c)^2. From a theoretical point of view, this selection discriminates against the unwanted contribution from the neglected baryon exchange graph fig. 2d, as well as other amplitudes possibly involving exotic exchange. For $M(K^{*-}\pi^+) < 1.3$ GeV, there are 665 events in this restricted t_{pn} region, compared with a total of 1050 in the same mass region if no selection is imposed on t_{pn}.

The mass distribution $d\sigma/dM_{K^*\pi}$ is shown in fig. 6. A pronounced K*(1420) peak is seen above a broad background. The $J^P = 2^+$ K*(1420) is known to be produced, in large measure, by π exchange coupling at the pn vertex. We do not attempt to describe this resonance production here but concentrate on the "background" under this signal. The solid curve in fig. 6 shows the shape of the $K^{*-}\pi^+$ mass spectrum predicted by our model. The curve is normalized to data in the region $M(K^*\pi) <$ 1.28 GeV.

To avoid the influence of the K*(1420), which is not included in our model, detailed comparisons of momentum transfer and angular distributions are made only for events restricted to the near threshold region $M(K^{*-}\pi^+) \leq 1.3$ GeV. Because there is also a significant Δ^+ signal in the data which is not built into the model, we further eliminate events for which $M(N\pi^+) \leq 1.34$ GeV. In addition to the t_{pn} re-

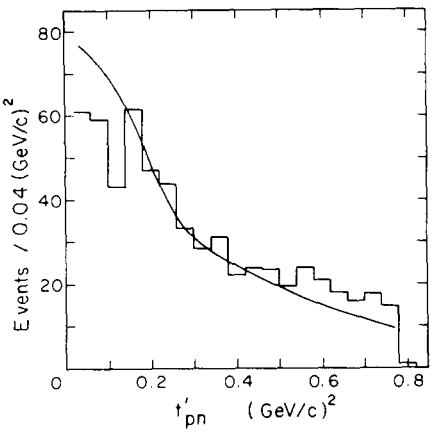

Fig. 7. Momentum transfer distribution in t'_{pn} for $K^- p \to K^{*-} \pi^+ n$ at 4.2 GeV/c obtained from the event sample with $M(K^*\pi) \leq 1.3$ GeV, $|t_{pn}| \leq 0.8$ (GeV/c)^2, and $M(n\pi^+) \geq 1.34$ GeV. The same selections were applied in obtaining the theoretical curve, based on eq. (2.12) of the text. The theoretical curve is normalized to the data.

striction described above, these are the only kinematic selections made.

In fig. 7, we present the production momentum transfer distribution, $d\sigma/dt'_{pn}$. The data fall roughly as $\exp(-3\, t'_{pn})$. This slow fall is reproduced adequately by the model. By contrast, a standard pion exchange Deck model provides a much sharper ($\sim\exp(-7\, t'_{pn})$) fall-off. The agreement of the model with data supports the need for the A_2 exchange contribution in the t_1 channel.

In fig. 8, we examine the distribution $d\sigma/dt_{KK^*}$ in momentum transfer between incident K and final K*. The distribution is broad, and again, it is reproduced by the model. In fig. 9, we present distributions in various decay angles in the ($K^*\pi$) rest

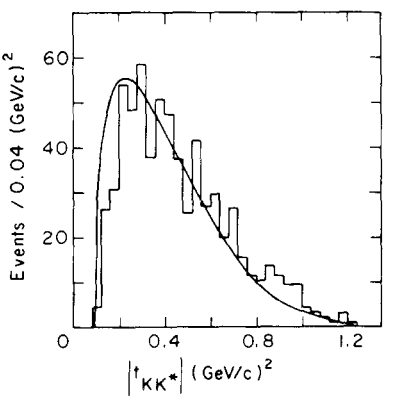

Fig. 8. Distribution in t_{KK^*}, with the same selections as in fig. 7.

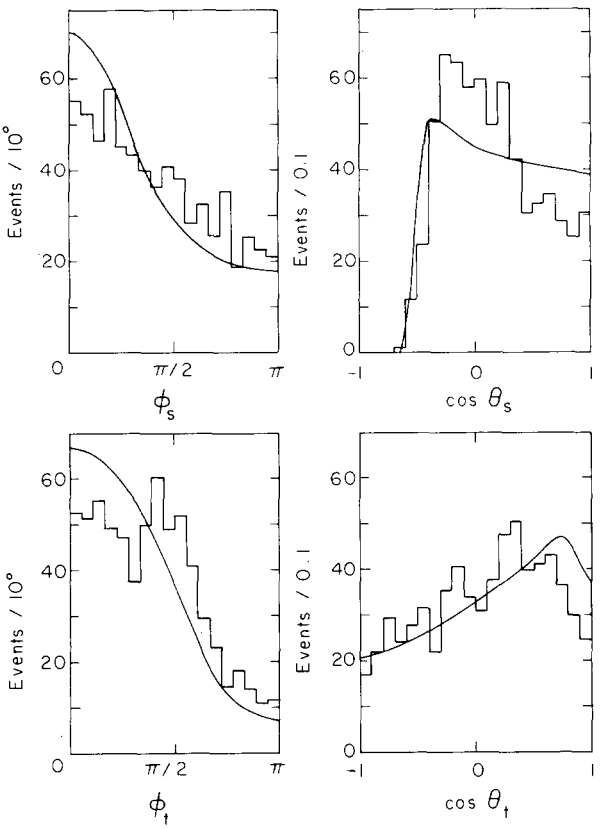

Fig. 9. Distributions in the decay angles of the K*, as measured in the (K*π) rest frame. (a) *s*-channel azimuthal angle. (b) Cosine of the *s*-channel polar angle. (c) *t*-channel azimuthal angle. (d) Cosine of the *t*-channel polar angle. The selections made for fig. 7 also apply here.

frame. We note, in particular, that the model reproduces the peaking of $d\sigma/d\phi_s$ towards $\phi_s = 0$. It was pointed out that this ϕ_s angle is crucial for attempts to identify exchange contributions [3]. The peak near $\phi_s = 0$ is correlated with the presence of peripheral exchanges at the KK* vertex of fig. 1. In our model these are the (π, π_x, η, and B) exchanges. The absence of a peak near $\phi_s = \pi$ in the data is consistent with the expected absence of exchanges in the (exotic) $K^-\pi^-$ channel.

In an attempt to verify the model in more detail, we select events in the small t_{KK^*} range defined by $|t_{KK^*}| \leqslant 0.3$ (GeV/c)^2. These events form a relatively purified sample of π exchange events. Distributions in t'_{pn}, and in the decay angles, from this restricted sample are displayed in figs. 10 and 11. The theoretical curves continue to follow the data nicely. No optimization of parameters is involved in this work. All curves are normalized to data.

We note that the rough agreement with the experimental decay angular distribu-

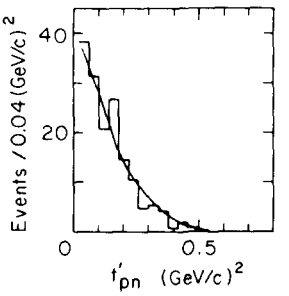

Fig. 10. Distribution in t'_{pn} for events satisfying the selections $M(K^*\pi) \leq 1.3$ GeV, $M(n\pi^+) \geq 1.34$ GeV, and $|t_{KK^*}| \leq 0.3$ (GeV/c)^2.

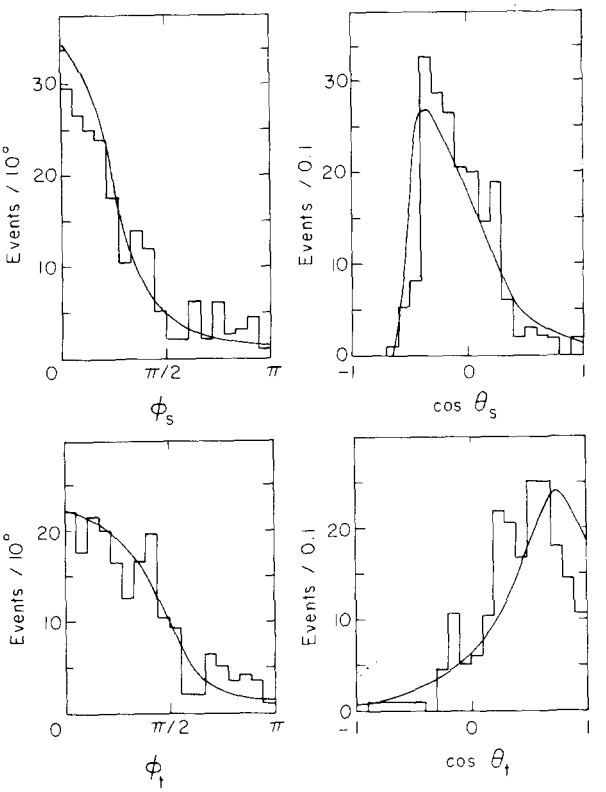

Fig. 11. Distributions in the decay angles of the K^* in the $(K^*\pi)$ rest frame for events satisfying the selections listed in the caption of fig. 10.

tions means that the spin-parity content of the decay is correctly embodied in the model, at least when averaged over the region $M(K^*\pi) \leqslant 1.3$ GeV. We may note in ref. [2], however, that there are unnatural parity exchange amplitudes as well as natural parity ($K\pi\pi$) states included in the data sample, which are not embodied in the model.

4. Conclusions

We have constructed a simple doubly peripheral exchange model for the process $K^-p \to K^{*-}\pi^+n$. The model satisfies the requirements of duality and incorporates exchange degenerate exchanges in both t channels. One of the four contributing amplitudes in the model is the $\pi\rho$ graph of the standard Deck model. However, we show that theory and data demand the presence of the other amplitudes. Duality specifies the relative magnitudes and phases of these four terms, so that our final amplitude includes no more free parameters than the usual Deck amplitude. In parametrizing our amplitudes, we have employed the Regge phases demanded by the analyticity properties of the two-reggeon one-particle vertex.

A comparison of theoretical distributions with 4.2 GeV/c data in sect. 3 shows a reasonable agreement. It would be valuable to compare the model with higher-energy data on the same process. Although the statistics of available higher-energy data are limited, the distribution $d\sigma/dt'_{pn}$ at 10 and 14 GeV/c is reported to fall roughly [9] as $\exp(-5\ t'_{pn})$, in good agreement with our calculation at these energies (fig. 5).

The data support the theoretical suggestion that both ρ and A_2 exchange contributions in the t_{pn} channel play an important role in the non-quasi-two-body reaction $K^-p \to (K^{*-}\pi^+)n$. The relative magnitude of these terms is specified theoretically by duality and (broken) exchange degeneracy. These theoretical expectations lead to a distribution $d\sigma/dt_{pn}$ which agrees with data. A much greater or much smaller ratio of ρ/A_2 would not be tolerable.

The ρ exchange term is identified with the usual charge-exchange Deck amplitude. Thus, our demonstration that an A_2 term is required is a further indication of the inadequacy of the usual Deck approach based on dominance of the $\pi\rho$ graph. A reevaluation is in order of the apparent success of the π exchange Deck model in the "diffractive" situations $K^{\pm}p \to (K^*\pi)^{\pm}p$. We note that in the diffractive case, the pion-exchange Deck model includes contributions from the πP, πf, and $\pi\rho$ pairs of exchanges. In our new model, one would want to include, in addition, $B\omega$ and BA_2 terms. The role of these extra terms in the diffractive case is much less significant than in charge exchange, however. This is true because the overwhelming term in the diffractive case is πP, which is absent in charge exchange. Moreover, the magnitude of the $B\omega$ and BA_2 contributions are reduced relative to πf and $\pi\rho$ because the B pole position is relatively far from the scattering region. In charge exchange, the corresponding ηA_2 term is more significant. Nevertheless, some effect on predicted cross-over behavior and polarization [3] may be expected from inclusion of

the $B\omega$ and BA_2 contributions [10], because the cross-overs and polarizations are a manifestation of interference between the secondary exchanges and the leading πP term. It will be noted that all these issues are more difficult to resolve cleanly in the diffractive case because, in addition to the "t-channel" exchange graphs (π, B), there are also "u-channel" exchange graphs. These K^* terms are absent in charge exchange, as described in sect. 2.

The success of our approach encourages further attempts to formulate equally simple double exchange models for other non-diffractive $2 \to 3$ particle reactions. We have in mind, for example, $K^- p \to \rho\pi\Lambda$.

E.L. Berger is grateful for the warm hospitality of the CERN Theoretical Physics Division and benefitted from conversations with A. White, G.C. Fox, and C. Sorensen.

References

[1] E.L. Berger and P. Pirilä, Phys. Rev. D12 (1975) 3448.
[2] Amsterdam-CERN-Nijmegen-Oxford Collaboration, Spin-parity structure of the $(\bar{K}\pi\pi)^0$ system produced in the charge-exchange reaction $K^- p \to (\bar{K}^0\pi^+\pi^-)n$ at 4.2 GeV/c, J.S.M. Vergeest et al., report HEN-145-3, submitted to Phys. Letters.
[3] E.L. Berger, Argonne Report, ANL-HEP-75-06, in Daresbury Meeting on three-particle phase-shift analysis and meson resonance production, ed. J.B. Dainton and A.J.G. Hey.
[4] E.L. Berger, Argonne report ANL-HEP-75-32, Proc. 6th Int. Colloq. on multiparticle reactions, Oxford, 1975.
[5] R.J. Hemingway, in New directions in hadron spectroscopy, ed. S. Kramer and E.L. Berger, Argonne report ANL-HEP-CP-75-58, p. 28.
[6] G.F. Chew and A. Pignotti, Phys. Rev. Letters 20 (1968) 1078.
[7] Particle Data Group, Phys. Letters 50B (1974) 1.
[8] R. Brouwer, C. De Tar and J. Weis, Phys. Reports 14 (1974) 257.
[9] Aachen-Berlin-CERN-London-Vienna and Athens-Democritus-Liverpool-Vienna Collaboration, G. Otter et al., Nucl. Phys. B84 (1975) 333.
[10] G. Cohen-Tannoudji, A. Santoro and M. Souza, Nucl. Phys. B95 (1975) 445.
[11] Amsterdam-CERN-Nijmegen-Oxford Collaboration, The reaction $K^- p \to \bar{K}N$ at 4.2 GeV/c, paper submitted to Int. Conf. on high-energy physics, Palermo, 1975.